Monochromatic X-Ray Sampling Imager for Laser-Imploded Core Plasma Observation with Highly Spatial, Temporal, and Spectral Resolutions

Minoru TANABE, Hiroaki NISHIMURA, Shinsuke FUJIOKA, Hiroki ISHIMARU, Yuichi INUBUSHI, Keiji NAGAI, Hiroyuki SHIRAGA, Takayoshi NORIMATSU, Hiroshi AZECHI and Kunioki MIMA

Institute of laser engineering, Osaka University, Osaka 565-0871, Japan

A novel x-ray imaging method, providing spatial resolution of 10 μm, temporal resolution 10 ps, and spectral resolution of $E/\Delta E = 200$ (*E*: photon energy), is suggested to diagnose laser driven fusion plasma. This scheme consists of a monochromatic x-ray imager with the use of two-dimensional (2D) curved crystals and an image-sampling streak camera. Feasibility of the method was studied using GEKKO XII laser and chlorinated plastic shell targets. Early appearance of Cl-Heα line emission during the implosion stage was found for the present conditions, which made image reconstruction difficult.

1. Introduction

In fast ignition scheme [1], dense plasma formation and additional heating with an ultra-short high-energy laser pulse are of great importance. In particular, the heating process was found to occur in a time window of 50 ps [2], implosion dynamics and energy transport process by fast particles must be investigated with x-ray spectroscopy and imaging of high resolutions in order to attain efficient fusion burn. Particle diagnostics, nominally used in the implosion experiment, are not suitable for such measurements because of poor temporal and spatial resolutions. We have measured the electron temperature and density profiles of laser-imploded core plasma generated upon the central spark scheme by observing x-ray line emissions from a tracer material doped in the target. In this case, spatially, temporally, and spectrally resolved images have been obtained with a monochromatic x-ray framing camera (M-XFC) [3], and the electron temperature and density profiles in the core plasma were derived for the first time [4]. In this method, an array of 2D curved crystals focused core plasma images on a photocathode strip line of x-ray framing camera. Temporal resolution of 35 ps with a frame interval of 50 ps was attained. But the resolutions are not sufficient to observe phenomena occurring in the process of fast ignition. Another scheme, consists of a multi-pinhole mask, a flat crystal, and an x-ray framing camera, inherently involves this problem although crystal alignment procedure is substantially simplified [5]. Therefore, a novel x-ray monochromatic imager capable

of high temporal-resolution has been expected without any time-intervals between images to obtain continuously and rapidly changing density and temperature profiles of the core plasma. We are developing a new type of monochromatic x-ray 2D image-sampling method, which allows the core plasma observation with high spatial-, temporal- and spectral-resolutions simultaneously.

2. Monochromatic Sampling Image X-Ray Streak Camera (Monochro-SIXS)

The new instrument consists of two toroidally bent Bragg crystals and a 2D sampling image x-ray streak camera (2D-SIXS) [6] as shown in Fig. 1. Monochromatic im-
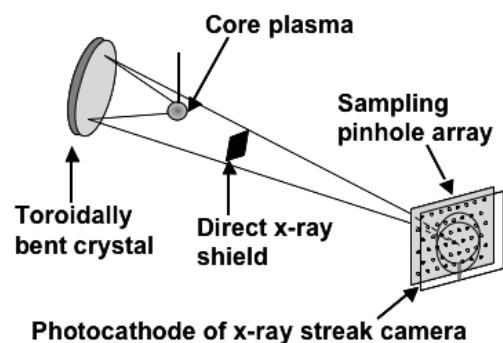
Fig. 1 Schematic view of monochromatic sampling image x-ray streak camera (Monochro-SIXS).

Table 1 Specifications of the two monochromatic imagers.

Objective x-ray line	Cl^{15+} Heβ	Cl^{16+} Lyβ
Photon energy (keV)	3.272	3.508
Bragg Crystal	Si (220)	Q (11.2)
Bragg angle (deg.)	80.7	76.4
Bending radii (mm)	200/195.8	200/189.5
Spectral window (eV)	11.7	26.2
Magnification	25.8	26.2
Target-Crystal (mm)	102.5	100.9
Crystal-Detector (mm)	2648.2	2640.7

Fig. 2 Micrograph image of the sampling mask.

ages of two different lines are focused onto an extended photocathode of the x-ray streak camera (XSC). The use of toroidally bent crystals, as an imaging device, has several advantages in keV x-ray imaging. High collection efficiency for x-ray photons can be obtained because of a much larger collection angle than those with conventional imager such as an x-ray pinhole camera. Spectrally narrow window enables us to identify plasma position. In particular, toroidally bent crystals reduces astigmatism in image by optimizing crystal curvatures for a given photon energy [7]. This is in contrast to the case of spherically curved crystals [8], which provide images at limited choice of photon energy to avoid large astigmatism.

In this scheme , we have chosen chlorine as a tracer material, and Cl^{15+} Heβ and Cl^{16+} Lyβ lines were respectively imaged by using Si (220) and Quartz (11.2) crystals. Specifications of the crystals are listed in Table 1. Each crystal has a Be filter of 100 μm in thickness to shield plasma debris. The crystals are mounted on miniature goniometers with six freedoms of adjustments. After the crystal alignment with visible light, the crystals were slightly tilted by referring angular differences between the visible light and x-ray measurement. The angular difference arises because the crystal lattice plane is not always in parallel to the crystal device surface. The difference is typically 0.1 degrees. The distance from the plasma to the crystal was around 10 cm and that from the crystal to the photocathode of XSC was around 260 cm. Thus image magnification was about 26.

An image-sampling mask was set in front of the XSC's photocathode with the separation distance of 1 mm. The mask has pinhole array of 52 × 85 on a Ni foil of 25 μm in thickness. The size of pinhole, fabricated with photolithographic method, was 45 ± 5 μm (see Fig. 2). The distance between the pinhole array along the space direction was 260 μm. Spatial resolution predicted with the sampling theory was 20 μm. Temporal resolution, defined by the pinhole size and the sweep speed of XSC, was 50 ps. The pinhole separation of 520 μm along the sweep direction allows an observation time window of 500 ps. Note here that these parameters were not optimized for practical implosion experiments yet. Combination of higher sweep speed and larger image-magnification leads to a temporal
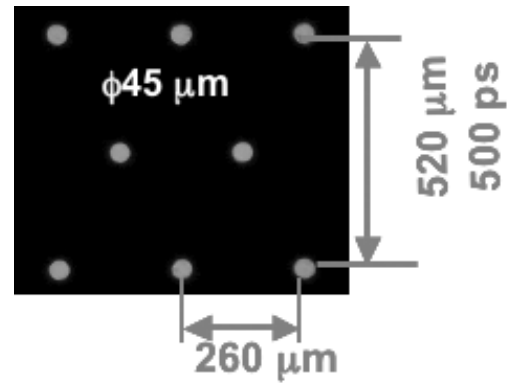
resolution better than 10 ps and a spatial resolution better than 10 μm.

The XSC used in the experiments was HAMA-MATSU C2590 including a streak tube with electrostatic focus lens. The photocathode was Au of 0.03 μm in thickness coated on a $C_{10}H_8 O_4$ foil of 3 μm in thickness. The size of the photocathode was 16 mm × 25 mm. Overall spatial resolution on the photocathode is nearly 200 μm for this XSC. Note here that if we use an x-ray streak camera using a streak tube with electromagnetic focus lens [9], the resolution on the photocathode of 100 μm can be attained.

3. Implosion Experiments

The Monocho-SIXS was attempted in GEKKO XII laser driven implosion experiments to address issues in this approach. A triple layered chlorinated plastic shell was irradiated with twelve beams of 526 nm in wavelength and 4.03 kJ in total energy. To homogenize laser intensity distribution on the target, random phase plates (RPP) were used. Laser energy imbalance among the beams was better than 5 %. The laser beams were focused at $d/R = -5$, where R is the shell radius and d is the distance form the shell center to the laser focus point, d is defined as positive when a laser beam is focused in front of the shell center.

The shell target of 500 μm in diameter consisted, from the inside to the outside, of 2 μm-thick C_8H_7Cl layer, 5 μm-thick CH ablator, and 0.03 μm-thick aluminum overcoat. The overcoat is important to avoid so-called "shine-through". It means that, in very early stage of plasma formation, laser light shines through transparent plastic layer, if any, so that it can cause localized plasma heating. This effect can be a seed of fluctuations for hydrodynamic instabilities during the implosion and stagnation processes.

An x-ray streak spectrograph (XSS) with a flat RbAP (100) crystal was used to observe temporal variation of Cl K-shell line emissions ranging from 2.5 to 3.5 keV. Time resolution was 28 ps and the energy resolution including source extent was 9.6 eV near Cl^{15+} Heβ line. An x-ray pinhole camera (XPHC) coupled with a charge-coupled-device (CCD) was used as a monitor of plasma

generation. Image magnification was 9 and spatial resolution was 21 μm. An 11 μm-thick Saran Resin filter (CH_2-CCl_2)$_n$(CH_2-$CHCl$)$_m$ was used in XPHC-CCD to record quasi-monochromatic x-ray images particularly for Cl-Heα line at 2.79 keV with a 0.05 keV bandwidth.

4. Experimental Results and Discussion

Figure 3 shows the results for Cl-Heβ line emission obtained with Monocro-SIXS. The upper figure (a) is a static (i.e. no-sweep) image when a C_2H_3Cl plate of 200 μm in thickness was irradiated with one beam from GEKKO XII without RPP. It is seen that the dot images are distributed widely. That corresponds to expanding plasma toward the incident laser. Mainly due to imperfect image transfer in the streak tube, boundary of each image is not distinct. Such image burrying is not seen when x-ray streak camera with an electromagnetic focus tube is used [9]. The lower figure (b) is streaked image when the shell implosion was made. Stripe structures, we expected, were not clearly observed and they appear to be overlaid each other. This overlay is partly due to the burry image but mainly due to much longer duration of Heβ line emission than that predicted by computer simulation.

Figure 4 (a) shows a flow diagram of the chlorinated shell implosion and waveform of absorbed pulse. This simulation was calculated with ILESTA 1D radiation hydrodynamic code assuming perfect spherical convergence
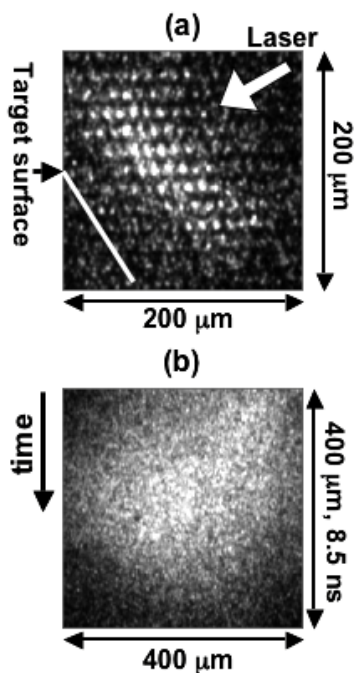
[10]. Figure 4 (b) shows comparison of Cl-Heβ line emission history measured with XSS and that predicted with ILESTA simulation. The temporal radiation of Heβ line emission was represented by the spectral emission ranging from 2.7-3.7 keV since the atomic model included ILESTA is the screened-hydrogenic, average ion model. As is seen in the comparison the experimental emission starts much earlier than the prediction. And that overall emission time was 1.1 ns at the signal foot, which was much longer than the designed time window of 500 ps and the predicted emission duration of 100 ps. In fact, the quasi-monochromatic XPHC image shown in Fig. 5 infers the early appearance of Heβ line emission. The core emission of approximately 100 μm in diameter was surrounded by a ring-like emission of 250 μm in diameter. This infers that the ring emission started at the intermediate stage of shell implosion. Namely, CH ablation layer was too thin for the present condition to emit Cl-Heβ line only when the chlorinated layer is stagnated at the center. As a result, the tracer layer was exposed in the ablation layer during the implosion stage and is directly heated by laser. Such a higher mass ablation rate than prediction might be caused by combination use of RPP and coherent laser light. The interference speckles caused by the combination lead to much higher local irradiance than the average. These are inherently unavoidable unless partially coherent light (PCL) [11] or smoothing by spectral dispersion (SSD) technique [12] is used. Furthermore, the local heating can also be a seed of perturbation for hydrodynamic instabilities. In this way, adoption of an XSC with electromagnetic focus lens and much uniform laser irradiation will be necessary to demonstrate feasibility of Monochro-SIXS. In

Fig. 3   X-ray images obtained with Monochro-SIXS. (a) Static image of Cl-Heβ line emission from a C_2H_3Cl plate. (b) Streaked images of Cl-Heβ line emission from laser imploded chlorinated shell.
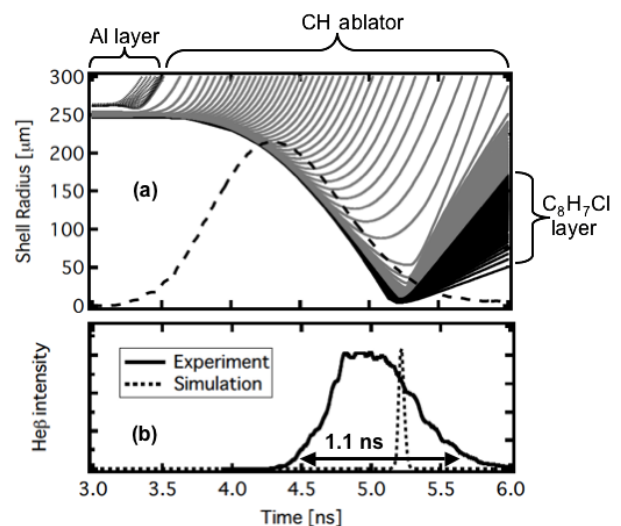

Fig. 4   (a) Flow diagram of the chlorinated plastic shell implosion and temporal variation of absorbed laser pulse (dotted line) simulated with ILESTA 1D. (b) Comparison of the experimental Heβ line emission (solid line) with the simulation (dotted line).
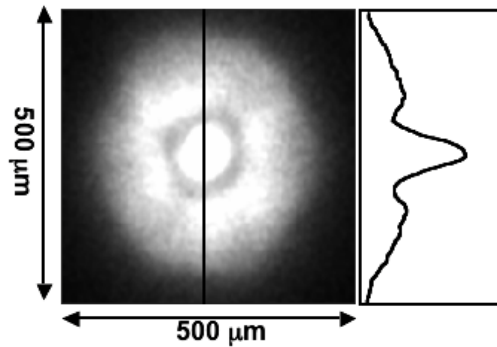
Fig. 5 Time-integrated, quasi-monochromatic image obtained with XPHC, and its lineout at the center. The ring-like emission seen around the core infers early appearance of Cl-Heα line emission.

addition, a new type of target can be suggested. For example, a gas-fill shell target suppresses hydrodynamic instabilities occurring in the implosion stage because the imploding shell is hydodynamically stable when higher density material compresses lower density material.

5. Conclusion

A novel scheme of monochromatic x-ray imager has been proposed, allowing temporal-resolution of 10 ps, spatial-resolution of 10 μm, and spectral-resolution of that normally obtained with Bragg crystals. We have made feasibility study using Gekko XII laser system and chlorinated plastic shells. The Cl-Heβ emission images obtained with Monochro-SIXS were overlaid each other because of the earlier appearance of tracer emission than that predicted. The experimental result infers that the hydrodynamic instability occurs during the implosion process. Further study is undertaken to improve image quality to demonstrate the designed value for practical use of this method in fast ignition experiments.

Acknowledgments

[1] M. Tabak, J. Hammer, M.E. Glinsky, W.L. Kruer, S.C. Wilks, J. Woodworth, E.M. Campbell, M.D. Perry and R.J. Mason, Phys. Plasmas **1**, 1626 (1994), R. Kodama, P.A. Norreys, K. Mima, A.E. Dangor, R.G. Evans, H. Fujita, Y. Kitagawa, K. Krushelnick, T. Miyakoshi, N. Miyanaga, T. Norimatsu, S.J. Rose, T. Shozaki, K. Shigemori, A. Sunahara, M. Tampo, K.A. Tanaka, Y. Toyama, T. Yamanaka and M. Zepf, Nature **412**, 798 (2001).

[2] R. Kodama, H. Shiraga, K. Shigemori, Y. Toyama, S. Fujioka, H. Azechi, H. Fujita, H. Habara, T. Hall, Y. Izawa, T. Jitsuno, Y. Kitagawa, K.M. Krushelnick, K.L. Lancaster, K. Mima, K. Nagai, M. Nakai, H. Nishimura, T. Norimatsu, P.A. Norreys, S. Sakabe, K.A. Tanaka, A. Youssef, M. Zepf and T. Yamanaka, Nature **418**, 933 (2002).

[3] I. Uschmann, K. Fujita, I. Niki, R. Butzbach, H. Nishimura, J. Funakura, M. Nakai, E. Förster and K. Mima, Appl. Opt. **39**, 5865 (2000).

[4] Y. Ochi, I. Golovkin, R. Mancini, I. Uschmann, A. Sunahara, H. Nishimura, K. Fujita, S. Louis, M. Nakai, H. Shiraga, N. Miyanaga, H. Azechi, R. Butzbach, E.F"orster, J. Delettrez, J. Koch, R.W. Lee and L. Klein, Rev. Sci. Instrum. **74** 1683 (2003).

[5] J.A. Koch, T.W. Barbee, Jr., N. Izumi, R. Tommasini, R.C. Mancini, L.A. Welser and F.J. Marshall, Rev. Sci. Instrum. **76** 073708 (2005).

[6] H. Shiraga, M. Nakasuji, M. Heya, and N. Miyanaga, Rev. Sci. Instrum. **70** 620 (1999).

[7] M. Vollbrecht, I. Uschmann, E. Förster, K. Fujita, Y. Ochi, H. Nishimura and K. Mima, J. Quant. Spectrosc. Radiat. Transfer. **58**, 965 (1997).

[8] Y. Aglitskiy, T. Lehecka, S. Obenschain, S. Bodner, C. Pawley, K. Gerber, J. Sethian, C.M. Brown, J. Seely, U. Feldman and G. Holland, Appl. Opt. **37**, 5253 (1998).

[9] See, for example, Hamamatus C7700-31.

[10] H. Takabe, M. Yamanaka, K. Mima, C. Yamanaka, H. Azechi, N. Miyanaga, M. Nakatsuka, T. Jitsuno, T. Norimatsu, M. Takagi, H. Nishimura, M. Nakai, T. Yabe, T. Sasaki, K. Yoshida, K. Nishihara, Y. Kato, Y. Izawa, T. Yamanaka and S. Nakai, Phys. Fluids **31**, 2884 (1988).

[11] H. Nakano, K. Tsubakimoto, N. Miyanaga, M. Nakatsuka, T. Kanabe, H. Azechi, T. Jitsuno and S. Nakai, J. Appl. Phys. **73**, 2122 (1993).

[12] S. Skupsky, R.W. Short, T. Kessler, R.S. Craxton, S. Letzring and J.M. Soures, J. Appl. Phys. **66**, 3456 (1989).